

PHOTOCATALYTIC DEGRADATION OF METHYLENE BLUE ON NANOSTRUCTURED COMPOSITES BASED ON TiO₂-Bi₂O₃

*Igor KOBASA

Department of Analytical Chemistry, Chernivtsi National University, Kotsiubinsky St., 2, Chernivtsi
58012, Ukraine. E-mail: imk-11@hotmail.com

*Corresponding author

Received 7 September 2011, accepted 15 November 2011

Abstract. *Oxide systems based on mixtures TiO₂-Bi₂O₃ with various quantitative and phase compositions have been synthesized and their light absorption spectra were analyzed. These systems can reveal the quantum dimensional effects and exhibit photocatalytic activity in the reaction of photodegradation of methylene blue (MB). A complex investigation of the structure, spectral and photochemical properties of the oxide systems proved that low concentration of the dope (0.01-0.1 wt % of Bi(III)) causes rise in the light absorption value and higher intensity of the MB photodegradation. Further rise in the Bi(III) concentration results in formation of the amorphous Bi₂O₃ and decrease in the photocatalytic activity. An energy analysis of the oxide system has been provided and possible mechanism for the components interaction was proposed.*

Keywords: photocatalytic activity; TiO₂-Bi₂O₃; methylene blue; nanostructured composites, dye photodegradation

1. Introduction

Titanium dioxide and TiO₂-based oxide mixtures, are known as semiconductors, which reveal wide range of important and useful electrophysical and physico-chemical (photochemical, catalytic, photocatalytic) characteristics. These features promise many useful applications for such TiO₂ system [1-7]. For instance, they can be used to synthesize new products [8, 9], for neutralization of hazardous wastes and industrial gas emissions [10-12], photocatalytic and photoelectrochemical solar energy transformation [13-15], and for systems for information storage and transmission etc. [16-18]. Photocatalytic activity can be enhanced through development of new compositions, which include a semiconductor-photocatalyst and some additional compounds (another semiconductors, ions-modifiers, metal nanoparticles, etc.). Such composition ensures

more effective separation of the light-generated charges, which can be transported from the photocatalyst to the substrate. This process reduces efficiency of the recombination.

Therefore, a system TiO₂-Bi₂O₃, seems promising for potential applications in the water decontamination technologies, in the VIS-induced oxidation processes [19]. Activity of this system in degradation of 4-chlorophenol is higher than activity of the pure titania or P25 under the sunlight [20]. However, a generally recognized theory of an influence of the bismuth admixture on various properties of TiO₂, which determine the potential of application of titania as a functional material (catalyst, photocatalyst, energy convertor etc.) is not developed yet.

2. Experimental

We synthesized some TiO₂-Bi₂O₃ samples using one of the following methods.

First method supposed synthesis of metal hydroxides at the room temperature with further thermal processing and transformation of the hydroxides into oxides. Basic flowsheet of this method includes following stages: deposition of a metal hydroxide through adding of ammonia solution (5-10 %) to solution of the corresponding metal salt. Jelly-like deposit of the hydroxide forms after this operation, then it should be separated from the solution and washed to remove unreacted compounds. Then the deposit undergoes drying, heating to 600 °C to remove remainders of ammonia, calcination for formation and structuring of oxides (at 600 °C for about 6 hours), and, finally, the oxide products should be ground.

Another method supposed high temperature synthesis of the product and it was engaged to obtain some other TiO₂-Bi₂O₃ systems. Method of the pyrogenic synthesis of TiO₂ [21] was modified according to the following flowsheet. Source materials should be heated previously then TiCl₄ undergoes the high temperature hydrolysis and TiO₂ forms after this operation. At the beginning, all parent components (air, hydrogen and titanium tetrachloride) are mixed together in the combustion chamber at 70-100 °C and piped to the reactor. This mixture burns in the reactor and forms water. Temperature of the hydrogen-oxygen flame is high (700-1100 °C) and just-formed water causes hydrolysis, which runs in the burning zone. A solution of Bi(NO₃)₃ had been injected to the cooling zone of the reactor (t = 600-800 °C) through an additional sprayer. A highly disperse particles of TiO₂-Bi₂O₃ were formed in the cooling zone of the reactor as a result of these processes.

We have synthesized TiO₂-Bi₂O₃ samples containing 0.01; 0.1; 1.0; 5.0; and 10.0 mass % of Bi₂O₃. An atom-absorption spectroscopy was used to determine contents of Bi₂O₃.

Photocatalytic activity (PA) of the samples has been determined in the characteristic reaction of methylene blue (MB) reduction to its leucoform [22]. Electroconductivity (σ) of the samples has been determined using a direct current method and specific surface area was measured by BET method with low temperature adsorption of argon.

3. Results and Discussion

As it is seen from the data of Tab. 1, the samples with 0,1 mass % of Bi₂O₃ exhibit the highest level of photocatalytic activity in redox reaction. Besides that, pyrogenically synthesized samples exhibit much higher activity comparing to the samples, which were synthesized through low-temperature liquid phase deposition (see results 2, 3, 8, 9). Activity of the samples lowers at the rise of bismuth content and the samples with 10,0 mass % of Bi₂O₃ exhibit same level of photocatalytic activity as non-doped titanium dioxide. Pure bismuth oxide without dope of TiO₂ (see Tab. 1, example 7) exhibits very low level of photocatalytic activity in the redox reaction. This fact proved through four hours exposition of such a sample to UV radiation, which did not result any change in optical density of the methylene blue solution.

Analyzing data of Tab. 1, one can see that electroconductivity and photocatalytic activity of the samples are cymbatic while their PA does not exhibit such dependencies on the specific surface area. For instance, we have synthesized a 0,01 mass % doped sample with S_{spc} 2,5 times lesser than S_{spc} of the non-doped sample. However, PA and σ of the doped sample were 5,8; and 2,8 times correspondingly higher than the values of the non-doped sample. Dependence of PA on σ becomes even more obvious if we compare data for samples 3 and 6. They have the same specific area surface but various content of the dope (0,1 mass % for the sample 3 and 10,0 mass % for the sample 6) and σ . As a result, PA of the sample 6 substantially differs from the values of the sample 3. Therefore, comparison between values of σ and activity of the samples proves that quantity of free electrons, which present in the material, mainly governs its activity. The latter characteristic does not substantially depend on S_{spc} . Of course, it influences the activity but, in this case, not significantly.

Table 1
Photocatalytic (PA) activity, specific surface area (S_{spc}) and electroconductivity (σ) of $\text{TiO}_2\text{-Bi}_2\text{O}_3$ systems

Number	Bi_2O_3 mass %	S_{spc} , m^2/g	PA ($\text{mg}/(\text{ml min m}^2)$)	σ , S/cm
1	0	15	$8,3 \cdot 10^{-1}$	$9,63 \cdot 10^{-7}$
2	0,01	6	4,8	$2,65 \cdot 10^{-6}$
3	0,1	20	5,8	$7,95 \cdot 10^{-6}$
4	1,0	8	5,4	$3,22 \cdot 10^{-6}$
5	5,0	24	4,7	$2,55 \cdot 10^{-6}$
6	10,0	20	$9,0 \cdot 10^{-1}$	$9,85 \cdot 10^{-7}$
7	99,99	$1,0 \cdot 10^{-4}$	$1,82 \cdot 10^{-7}$	
8*	0,01	130	6,5	$9,12 \cdot 10^{-6}$
9*	0,1	55	7,3	$9,48 \cdot 10^{-6}$

* - flame hydrolysis synthesized samples

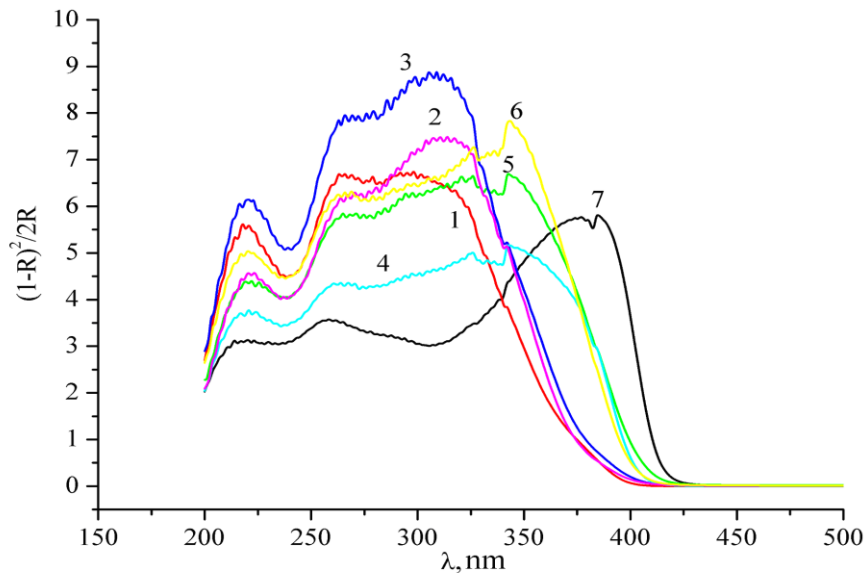


Figure 1. Absorption spectra for $\text{TiO}_2\text{-Bi}_2\text{O}_3$ systems. The spectra derived by Kubelka-Munk method from spectra of diffusion reflection (R , %) for: (1) – anatase with rutile admixtures; (2) – (6) co-deposition products containing mass % of Bi_2O_3 : 0,01 (2); 0,1 (3); 1,0 (4); 5,0 (5); 10,0 (6) and pure rutile (7)

The Kubelka-Munk method [23] of calculation of absorption spectra from the data of diffusive reflection spectra can bring important information about characteristics of $\text{TiO}_2\text{-Bi}_2\text{O}_3$ systems. As it is seen from Fig. 1 (see spectra 2 and 3), position of the absorption bands for 0,01 mass % and 0,1 mass % doped samples almost coincide with the position of non-doped TiO_2 band (see spectrum 1) while absorption intensity of the doped bands is higher. The most active sample (spectrum 3) also exhibits the highest rise of the absorption coefficient and, consequently, energy of the oscillator, which

determines probability of the electron jump to the conduction band.

Rise in bismuth content over 1,0 mass % causes significant spectral changes. A new absorption band with absorption maximum near 340 nm appears for the samples containing over 1,0 mass % of the dope. Absorption level of this band gradually raises as bismuth content rises to 5,0 and 10,0 mass % (see Fig. 1, spectra 4-6). In our opinion, these changes can be caused by formation of the new bismuth oxide phase. To verify this assumption, we recorded diffusion

reflection spectra for two Bi_2O_3 samples with various purity grades and derived absorption spectra from the previous ones. As seen from Fig. 2, a sample graded as “pure” generates spectrum, which is close to the shape of samples 4-6 spectra (see Fig. 1). However, there is a difference between them. Bismuth oxide samples spectra are bounded from the long wave edge at 438-442 nm (see Fig. 2) and these wavelengths correspond to $E_g = 2,81\text{-}2,83$ eV, which is very close to $E_g = 2,80$ eV [24]. As contrary to these values, the doped samples spectra (dope content is from 1,0, to 10,0 mass %) are bounded from the long wave edge at 403-405 nm (see Fig. 1), which corresponds to $E_g = 3,07$ eV. This fact gives us ground to suppose influence of quantum dimensional effects for Bi_2O_3 particles for the samples 4-6. This assumption was verified and proved through determination of the particles size range using Scanning electronic microscope ZEISS EVO 50XVP. Particles sizes were ranged from 10 to 20 nm for the samples 4-6.

Alternative explanation involving rutile-related long wave bands for the samples 4-6 should not be accepted because of the following. Our rutile samples (purity grade is “very pure”) spectra have another shape: there is a minimum at 310 nm and their long wave edge is bounded at 412 nm (see Fig. 1), which corresponds to $E_g = 3,01$ eV. This value is in agreement with the reference value $E_g = 3,02$ eV [1].

Then we investigated energetic parameters of $\text{TiO}_2\text{-Bi}_2\text{O}_3$ system basing on previous spectral data. This investigation stage was aimed to finding connection between changes in the photocatalytic activity depending on the dope content. As reported in [24], conductivity band of the regular (without any quantum dimensional effects) bismuth oxide corresponds to $E_{CB} = -4,83$ eV (referring to the absolute potential scale, which starts from the zero point in vacuum). Potential of the normal hydrogen electrode is $E^0 = -4,50$ eV in this scale, therefore, one

can recalculate the above E_{CB} into the normal electrochemical potential scale as $E_{CB} = +0,33$ V (referring to the normal hydrogen electrode).

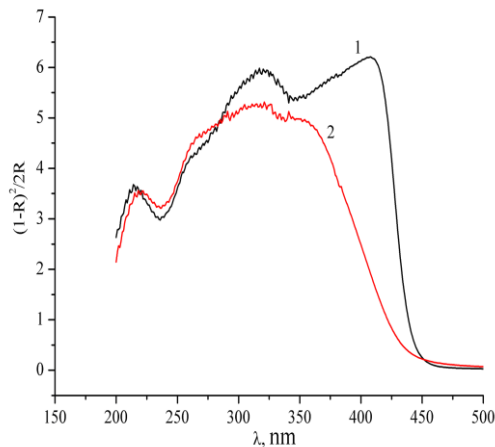


Figure 2. Absorption spectra for Bi_2O_3 materials: “pure” graded (1) and “pure for analysis” graded (2). The spectra derived from diffusion reflection spectra (R, %) by Kubelka-Munk method

The band-gap potential $E_g = 2,80$ eV and the valence band potential $E_{VB} = +3,13$ V should also be taken into consideration.

Further, we analyze influence of the quantum dimensional effects on the above potentials. There is a difference (see spectra in Fig. 1) between the band-gap width for the regular (E_g) and nano-sized ($E_{g(\text{nano})}$) particles of bismuth oxide obtained in experiments 4-6 and this difference is $\Delta E_\sigma = E_{\sigma(\text{nano})} - E_\sigma = 3,07 - 2,8 = 0,27$ eV. Theory of the quantum dimensional effects shows that both bands (conductivity and valence) shift because of the band-gap change. An “excessive” ΔE_σ distributes between the two bands inversely as to effective mass of electrons and holes (m_{e^*} and m_{h^*}). It has been found²⁵ that the conductivity band of n-type semiconductors is a subject of more substantial shift comparing to the valence band shift. We did not have any information regarding actual m_{e^*} and m_{h^*} and assumed the ratio between

contributions to E_{CB} and E_{VB} as 3:1. This assumption proceeded to values of $E_{CB} = +0,13$ V and $E_{VB} = +3,20$ V. We recalculated $E_{CB} = -4,12$ eV²⁴ to the electrochemical potential scale and obtained $E_{CB} = -0,29$ V in order to find position of the allowed energy bands. Then this potential was compared to $E_g = 3,20$ eV, which resulted $E_{VB} = 2,91$ V. An energy diagram for titanium oxide and both regular and nano-sized (with quantum dimensional effects) bismuth oxide is shown in Fig. 3. A dye reduction potential is also shown in the diagram.

Since potential of an electron injection to the conductivity band of the nano-sized bismuth oxide E_{CB} is more positive than potential of an electron transfer from photoexcited titanium oxide to the dye E_{MB/MB^-} , which results its reduction, both processes can be considered as competitive. Consequently, effect of an electron injection process increases as bismuth oxide content rises, which should promote decrease of PA.

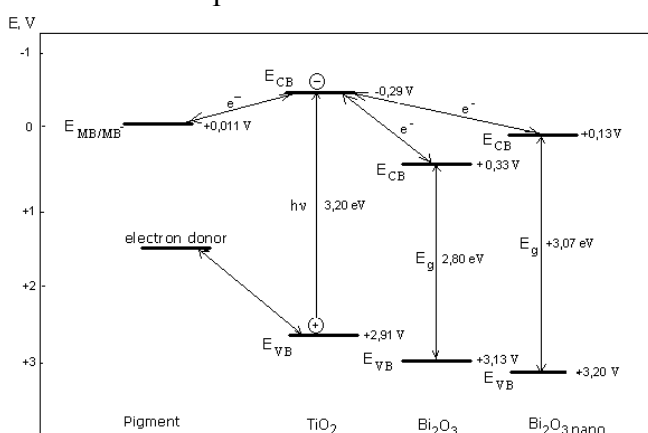


Figure 3. An energy diagram of titanium and bismuth oxides based system and scheme of the electron transfers at MB reduction

Indeed, data from Tab. 1 proves decrease of the photocatalytic activity for more than 6 times as Bi_2O_3 content increases from 1,0 to 10,0 mass % (samples 4-6). Further decrease of PA can be caused by increase of the particles size, which leads to gradual disappearance of the quantum

dimensional effects and widening of the energetic gap $\Delta E = E_{CB}(TiO_2) - E_{CB}(Bi_2O_3)$, which governs driving force of the process.

4. Conclusion

Results of investigation of the structure, electric and photocatalytic properties, thermodynamic analysis of the energy characteristics of the system $TiO_2-Bi_2O_3$ proved that this material can reveal quantum-dimensional effects and promote photoreduction of methylene blue.

5. References

- [1]. M. Grätzel (Ed), (1986). Energetic resources through a prism of photochemistry and catalysis, Mir, Moscow.
- [2]. M. Fox, M. T. Dulay, Heterogeneous photocatalysis. (1993). *Chem. Rev.* 193 341-357.
- [3]. M. R. Hoffmann, S.T. Martin, W. Choi, and D.V. Bahnemann., Environmental applications of semiconductor photocatalysis. (1995). *Chem. Rev.* 195 69-96.
- [4]. A. Mills and Le Hunte S., An overview of semiconductor photocatalysis. (1997). *J. Photochem. and Photobiol. A: Chem.* 108 1-35.
- [5]. A. Hagfeldt and M. Grätzel, Molecular photovoltaics (2000). *Acc. Chem. Res.* 33 269-275.
- [6]. A. Fujishima, X. Zhang, D. A. Tryk, TiO_2 photocatalysis and related surface phenomena. *Surface Science Reports.* (2008). 63 515-582.
- [7]. M. Grätzel, Conversion of sunlight to electric power by nanocrystalline dye-sensitized solar cells. (2004). *J. of Photochemistry and Photobiology A: Chem.* 164 3-14.
- [8]. K.T. Ranjit, T.K. Varadarajan, B.J. Visanathan, Photocatalytic reduction of dinitrogen to ammonia over noble-metal-loaded TiO_2 . (1996). *J. Photochem. and Photobiol. A: Chem.* 96 181-185.
- [9]. M. Anpo, H. Yamashita, Y. Ichihashi et al., Photocatalytic reduction of CO_2 with H_2O on titanium oxides anchored within micropores of zeolites: Effect of the structure on the active sites and the addition of Pt. (1997). *J. Phys. Chem. B.* 101 2632-2636.

- [10]. C. Nasr, K. Vinodgopal, L. Fisher et al., Environmental photochemistry on semiconductor surfaces. Visible light induced degradation of a textile diazo dye, naphthol blue black, on TiO₂ nanoparticles. (1996). *J. Phys. Chem.* 100 8436-8442.
- [11]. I. Poullos, M. Kositzi, A. Kouras, Photocatalytic decomposition of triclopyr over aqueous semiconductor suspensions. (1998). *J. Photochem. and Photobiol. A: Chem.* 115 175-183.
- [12]. Wang Chao, Ao Yanhui, Wang Peifang, Hou Jun, Qian Jin, Zhang Songhe, Preparation, characterization, photocatalytic properties of titania hollow sphere doped with cerium (2010). *J. Hazard. Mater.*, 178(1-3) 517-522.
- [13]. A.J. Bard, M.A. Fox, Artificial photosynthesis: solar splitting of water to hydrogen and oxygen. (1995). *Acc. Chem. Res.* 28 141-145.
- [14]. M. Ashokkumar, An overview on semiconductor particulate systems for photoproduction of hydrogen. (1998). *Internat. J. Hydrogen Energy.* 23 427-438.
- [15]. G.R. Bamwenda, S. Tsubota, T. Nakamura, M. Haruta, Photoassisted hydrogen production from a water-ethanol solution: a comparison of activities of Au—TiO₂ and Pt—TiO₂. (1995). *J. Photochem. and Photobiol. A: Chem.* 89 177-189.
- [16]. Sahyun M.R.V., Serpone N., Primary events in the photocatalytic deposition of silver on nanoparticles TiO₂ (1997). *Langmuir.* 13 5082-5088.
- [17]. Ch. Wang, Ch. Liu, et al., Spectral characteristics and photosensitization effect on TiO₂ of fluorescein in AOT reversed micelles (1998). *J. Colloid Interface Sci.* 197 126-132.
- [18]. I. Kobasa, I. Kondratyeva, L. Odosiy, TiO₂/biscyanine and CdS/biscyanine heterostructures: Influence of the structural composition on the photocatalytic activity. (2010). *Canadian J. of Chemistry.* 88(7) 659-666.
- [19]. Y. Bessekhoud, D. Robert, J. V. Weber, Photocatalytic activity of Cu₂O/TiO₂, Bi₂O₃/TiO₂ and ZnMn₂O₄/TiO₂ heterojunctions. (2005). *Catalysis Today*, 101 315-321.
- [20]. Xu Jing-jing, Chen Min-dong, Fu De-gang, Preparation of bismuth oxide/titania composite particles and their photocatalytic activity to degradation of 4-chlorophenol. (2011). *Trans. Nonferrous Met. Soc. China.* 21 340-345.
- [21]. I. M. Kobasa, J. W. Strus and M. A. Kovbasa, USA Patent WO/2009/052510. Method of Surface modifying titania using metal. (2009)
- [22]. I. M. Kobasa, Semi-conductive materials based on the titanium dioxide doped with zinc: Catalytic activity for copper deposition and effect of UV-irradiation. (2004). *Polish J. Chem.* 78 553-560.
- [23]. W.N. Delgass, C.L. Haller, R. Kellerman, J.H. Lunsford, (1979). Spectroscopy in heterogeneous catalysis. Academic Press, N.Y., San Francisco, London.
- [24]. Y. Xu., M. A. A. Schoonen, The absolute energy positions of conduction and valence bands of selected semiconducting minerals. (2000). *American Mineralogist.* 85 543-556.
- [25]. A. I. Kryukov, S. Ya. Kuchmii, V. D. Pokhodenko, Energetics of electron processes in semiconductor photocatalytic systems. (2000). *Theoret. and Exper. Chem.* 36 63-81.